Journal of Molecular Catalysis A: Chemical 318 (2010) 68–74

Contents lists available at ScienceDirect

Journal of Molecular Catalysis A: Chemical

journal homepage: www.elsevier.com/locate/molcata

Nanocrystalline ZSM-5: A catalyst with high activity and selectivity for epoxide rearrangement reactions

David P. Serrano[a,b,*], Rafael van Grieken[a], Juan Antonio Melero[a], Alicia García[a], Carolina Vargas[a]

[a] Department of Chemical and Environmental Technology, ESCET, Rey Juan Carlos University, c/ Tulipán s/n, 28933, Móstoles, Madrid, Spain
[b] IMDEA Energía, c/ Tulipán s/n, 28933, Móstoles, Madrid, Spain

ARTICLE INFO

Article history:
Received 2 June 2009
Received in revised form
12 November 2009
Accepted 12 November 2009
Available online 14 December 2009

Keywords:
ZSM-5
Nanocrystalline
Epoxide rearrangement

ABSTRACT

Nanocrystalline ZSM-5 (~20–50 nm) has been tested as a catalyst in the liquid phase rearrangement of 1,2-epoxyoctane, 2-methyl-2,3-epoxybutane and isophorone oxide together with a microcrystalline ZSM-5 sample (~5 μm) employed as a reference. Whereas this last material shows a low activity for the three epoxide rearrangement reactions considered, nanocrystalline ZSM-5 leads in all cases to high epoxide conversion. This different catalytic performance is attributed to the differences in the accessibility of the reactant molecules to the catalyst active sites. The smallest crystal size of the nanocrystalline zeolite contributes favourably to both the formation of a high external surface area, with no steric constraints, and to a faster intracrystalline diffusion of the epoxide molecules towards the acid sites located within the zeolite micropores. When sterically hindered epoxides are tested, the catalytic rearrangement occurs mainly on the external surface of the nanocrystalline zeolite. Moreover, it is remarkable that for the three epoxides investigated the high catalytic activity observed over nanocrystalline ZSM-5 is accompanied by the attainment of high selectivities, typically around or over 80%, towards products with commercial applications.

1. Introduction

Rearrangement of epoxides is a reaction commercially interesting as it allows the synthesis of useful intermediates for the chemical industry. The activation of epoxides through ring opening reactions can be catalyzed by Brönsted acid sites, *via* the addition of a proton to the epoxide oxygen, as well as by Lewis acid sites, *via* the coordination of the oxirane to a multivalent cation. A variety of products can be formed from those reactions depending on both the regioselectivity of the ring opening and the presence of steric constraints [1–3]. Both factors can be also adjusted by the convenient selection of the catalyst to be employed. A relatively large number of catalyst types have been used in the literature for epoxide rearrangement, including both homogeneous and heterogeneous systems. Among the latter, zeolites, metal oxides (e.g. silica and alumina), metal sulfates, and precipitated phosphates are the preferred ones [4–6]. First works related to aliphatic epoxides rearrangement over different zeolites were reported by Venuto and Landis (Na zeolites) [7], Imanaka et al. (HY zeolite) [8], and Matsumoto et al. (exchanged zeolites) [9,10].

Using zeolites as catalysts has the advantage of the existence of a well-defined pore system, which makes possible the control of the product distribution according to shape-selectivity effects. Likewise, depending on the type of zeolite, the acidic properties of the catalyst can be adjusted and varied according to the requirements needed in each reaction. Thus, zeolites in their proton form (e.g. H-ZSM-5) as well as the weakly Lewis-acidic Ti-silicate (TS-1) and Ti-Beta have been found to catalyze this type of reactions [11,12]. However, the best results have been obtained with aluminium-containing zeolites, as it is the case of zeolites X, Y, ZSM-5, Beta, and mordenite. These materials have been successfully tested in the rearrangement of aromatic and cyclic alkane epoxides, as well as of epoxides with tertiary carbons linked to the oxirane ring. Thus, high selectivities towards aldehydes have been obtained in the isomerisation of styrene oxide and derivatives over various acid zeolites [13,14]. Likewise, the rearrangement of cyclic α,β-epoxy ketones towards β-ketoaldehydes and diketones has been used for the preparation of pharmaceuticals, synthetic food flavourings and perfumes [15,16]. Meyer et al. reported the rearrangement of isophorone oxide with high yields (up to 80%) to keto aldehyde over zeolitic materials [17]. Likewise, some works have been published dealing with the use of zeolites as catalysts in the isomerisation of small size aliphatic epoxides, such as propylene oxide and 3-methyl-2,3-epoxybutane [18,19]. However, few results have been reported on the rearrangement of long straight-chain 1,2-alkane epoxides over zeolitic catalysts, probably due to

* Corresponding author at: Department of Chemical and Environmental Technology, ESCET, Rey Juan Carlos University, c/ Tulipán s/n, 28933, Móstoles, Madrid, Spain. Tel.: +34 91 664 74 50; fax: +34 91 488 70 68.
E-mail address: david.serrano@urjc.es (D.P. Serrano).

1381-1169/$ – see front matter © 2009 Elsevier B.V. All rights reserved.
doi:10.1016/j.molcata.2009.11.009

the low reactivity of these substrates and their bulky nature. A significant amount of different monounsaturated terminal alcohols is usually obtained in these reactions, along with other condensation products [20,21].

Since zeolites are microporous materials with small pore size, strong diffusional and steric hindrances usually occur when processing bulky molecules, and as a consequence, the activity of zeolites is then mainly originated by the active sites located on the external surface. Thereby, the external surface is a property of high relevance when the zeolite is intended to be used as a catalyst in reactions involving bulky compounds, such as polymer degradation, cracking of heavy oil fractions and fine chemicals production [22,23]. Thus, Wang et al. [24] have recently reported the catalytic performance of both nanoscale and microscale ZSM-5 in different reactions: toluene disproportionation, toluene alkylation with methanol and trimethylbenzene cracking. A superior reactivity was found over the nanoscale zeolite due its enhanced accessibility to acid sites.

In this context, nanosized zeolites with a considerable amount of fully accessible acid sites located on the external surface may be potentially interesting catalysts for rearrangement reactions involving large and long epoxides. Accordingly, in the present work, a comparison has been carried out between the catalytic behaviour of nanocrystalline and microcrystalline ZSM-5 samples for epoxide rearrangement reactions. In particular, the catalytic behaviour of these materials has been checked in the rearrangement of the three following epoxides: 1,2-epoxyoctane, 2-methyl-2,3-epoxybutane and isophorone oxide.

2. Experimental

2.1. Catalyst preparation

ZSM-5 zeolite with a micrometer crystal size (μ-ZSM-5) was prepared in presence of fluoride ions according to the procedure reported by Guth et al. [25]. Adequate amounts of tetrapropylammonium hydroxide (TPAOH, 40 wt.% aqueous solution from Alfa), deionized water and aluminium isopropoxide (AIP, 99 wt.% from Aldrich) were mixed under stirring at 25 °C, until a clear solution was obtained. Then, tetraethylorthosilicate (TEOS, 98 wt.% from Aldrich) was added to the solution and stirred during 40 h, the molar composition of the mixture being as follows: Al_2O_3:60 SiO_2:11 TPAOH:900 H_2O. Thereafter, hydrofluoric acid (HF, 48 wt.% aqueous solution from Panreac) was dropwise added with a molar ratio of HF/TPAOH = 1. The white gel obtained was transferred into PTFE-lined autoclaves and crystallized in static conditions at 170 °C during 5 days. The final solid product was separated from the remaining liquid phase by centrifugation at 11,000 rpm during 30 min, washed several times with distilled water and dried at 110 °C overnight. The calcined sample was obtained by treatment of the as-synthesized material in static air at 550 °C for 5 h.

Nanocrystalline ZSM-5 zeolite (n-ZSM-5) was prepared according to a procedure previously reported by van Grieken et al. [26]. Firstly, the aluminium source (aluminium isopropoxide, AIP, 99 wt.% from Aldrich) was added to an aqueous solution of tetrapropylammonium hydroxide (TPAOH, 40 wt.% aqueous solution from Alfa). The mixture was stirred at 0 °C to obtain a clear solution. Then, tetraethylorthosilicate (TEOS, 98 wt.% from Aldrich) was cooled down and added to the mixture under stirring at 0 °C. In order to achieve a total hydrolysis of the silicon species, the final solution was left under stirring during 48 h at room temperature. Thereafter, the ethanol formed was removed by vacuum heating at 45 °C. The concentrated solution was crystallized at 170 °C during 120 h in teflon-lined stainless-steel autoclaves. Finally, the solid product obtained was separated by centrifugation, washed several times with distilled water, dried overnight at 110 °C and calcined in air at 550 °C for 5 h.

2.2. Catalyst characterization

Crystallinity of zeolite samples was checked through X-ray diffraction (XRD) patterns acquired with a Philips X'PERT MPD diffractometer using Cu K_α radiation. Typically, the data were collected from 5 to 50° (2θ). The Si/Al atomic ratio of the samples was determined by induced coupled plasma-atomic emission spectroscopy (ICP-AES) with a Varian VISTA-AX equipment. Morphology and crystal sizes of both ZSM-5 zeolites were determined by SEM and TEM images. SEM photographs of conventional ZSM-5 zeolite were obtained using a PHILIPS XL30 ESEM.FEI scanning microscope operating at 20 kV, whereas TEM images of nanocrystalline n-ZSM-5 sample were obtained in a PHILIPS TECNAI 20 electron microscope operating at 200 kV.

Textural properties of catalysts were determined by means of nitrogen adsorption–desorption isotherms at 77 K with a Micromeritics ASAP 2010 porosimeter after outgassing of the calcined samples under vacuum at 200 °C for 5 h. The total surface area was determined according to the BET equation. The total pore volume was determined from the nitrogen adsorption at $p/p_0 = 0.99$. Micropore volume and external surface area of the catalysts were determined using the t-plot method [27]. The BJH model was employed for assessing the pore size distribution arisen from the intercrystalline voids of the n-ZSM-5 zeolite.

The coordination of aluminium atoms within the catalyst framework was checked by high resolution ^{27}Al MAS NMR spectra of the calcined samples. The spectra were recorded at 104.26 MHz using a VARIAN Infinity 400 spectrometer at spinning frequency of 4 kHz. Intervals of 30 s between successive accumulations were selected according to the structural nature of the samples. All the measurements were carried out at room temperature with $[Al(H_2O)_6]^{3+}$ as external standard reference.

The acid properties of the catalysts were determined by ammonia temperature programmed desorption (TPD) in a Micromeritics 2910 (TPD/TPR) equipment. Previously, the samples were outgassed under an He flow (50 N ml min^{-1}) by heating with a rate of 15 °C min^{-1} up to 560 °C and remaining at this temperature for 30 min. After cooling to 180 °C, an ammonia flow of 35 N ml min^{-1} was passed through the sample for 30 min. The physisorbed ammonia was removed by flowing He at 180 °C for 90 min. The chemically adsorbed ammonia was determined by increasing the temperature up to 550 °C with a heating rate of 15 °C min^{-1}, this temperature being maintained constant for 30 min. The ammonia concentration in the effluent He stream was monitored by a thermal conductivity detector.

2.3. Catalytic epoxide rearrangement experiments

The catalytic experiments were carried out in a stirred batch autoclave (0.1 L), equipped with a temperature controller and a pressure gauge, under stirring (550 rpm) and autogeneous pressure for 2 h. The reactor was also provided with a device to feed the epoxide into the teflon-lined reactor once the reaction temperature is reached. The solvent and the catalyst were initially placed in the Teflon-lined reactor. The zero time of the reaction was considered when the temperature reached the set-point value, the epoxide being then loaded into the reactor. The employed mass ratio epoxide/catalyst was 12 (1 g of epoxide and 80 mg of catalyst). Toluene was stored with zeolite A to minimise its water content (water content less than 0.04 wt.%). The catalyst, prior to the reaction, was dried overnight at 140 °C to remove adsorbed water, being subsequently transferred to the solvent-containing Teflon-lined reactor. This treatment is aimed to minimise and prevent the presence of

Table 1
Physicochemical properties of the ZSM-5 catalysts.

Catalyst	Si/Al[a]	Pore diameter (Å)	S_{BET} ($m^2\,g^{-1}$)[b]	$S_{EXT+MESOPOR}$ ($m^2\,g^{-1}$)[b]	D_c (nm)[c]	Acidity (meq g^{-1})[d]	T_{max} (°C)[d]
n-ZSM-5	32	5.5	384	70	20–50	0.59	353
μ-ZSM-5	35	5.5	340	8	5000–7000	0.63	342

[a] ICP-AES measurements.
[b] Nitrogen adsorption at 77 K.
[c] Mean crystal size.
[d] Ammonia TPD experiments.

water during the reaction as it may favour the formation of diols from the epoxide.

The reaction products were analyzed with a VARIAN 3800 gas chromatograph equipped with a capillary column (HP-FFAP) with dimensions 60 m × 0.32 mm, using a flame ionization detector (FID). Identification of the different reaction products was performed by mass spectrometry (VARIAN SATURN 2000) using standard compounds.

3. Results and discussion

3.1. Catalysts properties

The nanocrystalline ZSM-5 zeolite investigated in this work as a catalyst for the liquid phase rearrangement of different epoxides is featured by being formed by nanocrystals with a distribution of sizes in the range 20–50 nm. This fact provides this material with a high amount of fully accessible acid sites located on the external surface of the nanocrystals. Accordingly, this catalyst is considered to be potentially appropriate for the conversion of bulky molecules such as the epoxides selected in the present work. On the other hand, a sample of conventional microcrystalline ZSM-5 zeolite has been also prepared and tested as a catalyst in the liquid phase rearrangement of the different epoxides in order to be used as a reference.

As illustrated in Table 1, both ZSM-5 samples possess Si/Al molar ratios slightly higher than that corresponding to the synthesis gels (Si/Al = 30). XRD diffractograms in Fig. 1(a) show the typical pattern corresponding to pure MFI zeolitic structure for both samples. Nevertheless, the intensity of the peaks is lower in the nanocrystalline ZSM-5 which is consistent with the lower size of the crystals in this sample.

Fig. 1(b) illustrates the nitrogen adsorption isotherms at 77 K of both zeolite samples whereas Table 1 summarizes their textural properties. μ-ZSM-5 sample exhibits a predominantly type I isotherm, characteristic of purely microporous solids. In contrast, n-ZSM-5 showed a significant slope at intermediate relative pressures and a sharp increase for p/p_0 higher than 0.8 with well-defined hysteresis loop. This type of isotherm is characteristic of nanozeolites where adsorption takes place not only in the micropores but also with a significant contribution of the external surface and of the intercrystalline porosity. These aspects have also a pronounced effect on the textural properties of both ZSM-5 samples. Thus, owing to its smaller crystal size, n-ZSM-5 catalyst presents a larger external surface area (70 $m^2\,g^{-1}$) and a higher total pore volume (0.24 $cm^3\,g^{-1}$) than μ-ZSM-5 (8 $m^2\,g^{-1}$ and 0.14 $cm^3\,g^{-1}$, respectively). The presence of intercrystalline porosity in the n-ZSM-5 sample was confirmed by determining the mesopore size distribution using the BJH model (curve not shown). A relatively broad peak in the range 10–70 nm, with maximum at 25 nm, was so obtained, which agrees well with the size expected for the voids present between the nanocrystals in sample n-ZSM-5 (20–50 nm particle size).

As shown in Table 1, the average crystal sizes for μ-ZSM-5 and n-ZSM-5 zeolites, determined from SEM and TEM images, present

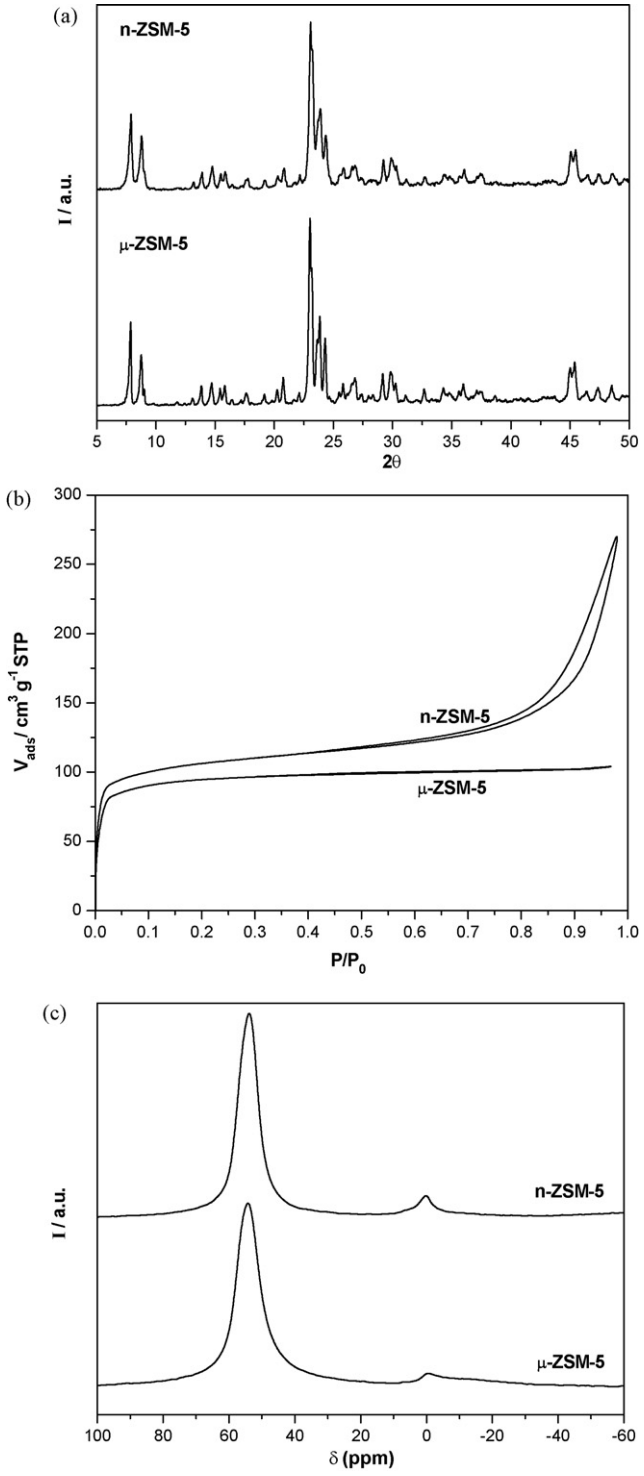

Fig. 1. Characterization of the ZSM-5 samples: (a) XRD patterns, (b) N_2 adsorption/desorption isotherms, (c) ^{27}Al-MAS NMR spectra.

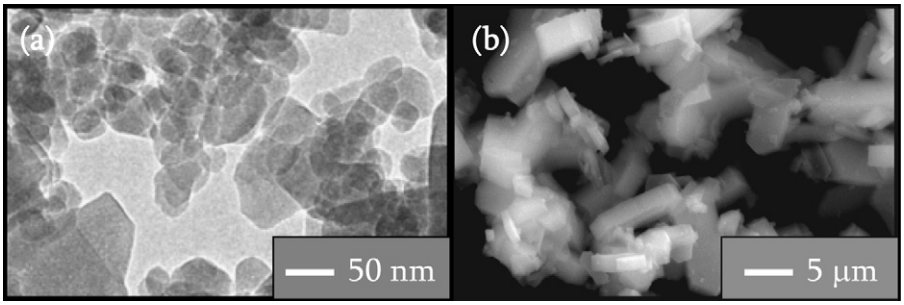

Fig. 2. TEM image of n-ZSM-5 sample (a) and SEM image of μ-ZSM-5 sample (b).

values around 5–7 μm and 20–50 nm, respectively (Fig. 2). This means that the size of the crystallites in n-ZSM-5 sample is about two orders of magnitude lower than in the μ-ZSM-5 material. As described above, the small crystal size of the nanocrystalline ZSM-5 contributes favourably to the formation of an extended external surface area and to a consequently higher share of external acid sites. Furthermore, a small crystal size should also reduce the diffusional hindrances for accessing the internal acid sites. Therefore, combination of both factors is expected to favour the accessibility of the molecules to the active sites in nanocrystalline zeolites.

^{27}Al-MAS NMR spectra of the two catalysts before calcination (not shown) present only a distinct peak at ~50 ppm, assigned to tetrahedral coordination, indicating that all the aluminium species are effectively incorporated into the zeolite framework. However, in the calcined samples, another small peak is detected, placed at ~0 ppm and assigned to octahedral (extraframework) aluminium species (Fig. 1(c)). These results indicate that even in the calcined samples most of the aluminium is effectively incorporated into the zeolite structure, while just a small proportion of aluminium is extracted from the framework during the calcination treatment.

The acidity of both zeolite samples has been investigated by NH_3 TPD experiments (see Table 1). The total amount of ammonia desorbed (meq g^{-1}) may be related to the number of acid sites whereas the temperature of the maximum in the desorption peak (T_{max}) provides an indication of the acid strength. The acidity values slightly change from one sample to another according to their different aluminium content: the Si/Al ratio is 32 for n-ZSM-5 and 35 for μ-ZSM-5. Likewise, a slight variation is observed in the temperature maximum for ammonia desorption corresponding to both ZSM-5 zeolite samples.

3.2. Catalytic epoxide rearrangement reactions

In order to compare the catalytic performances of both ZSM-5 samples in the liquid phase epoxide rearrangement, three epoxides having different molecular geometry and with commercial applications in fine chemistry have been selected as model compounds: 1,2-epoxyoctane, 2-methyl-2,3-epoxybutane and isophorone oxide. As a general rule, it has been observed that both ZSM-5 catalysts promote the isomerisation of the linear, branched and cyclic epoxides towards the corresponding ketones and aldehydes as main products through carbocation-mediated processes, although other secondary products are also detected.

The effect of the epoxide nature on the catalytic activity of the reaction, in terms of the epoxide conversion evolution along the time, is depicted in Fig. 3 for both catalysts. Because some epoxides may be isomerised thermally, blank reactions in absence of catalyst were carried out, yielding a very small conversion. These results show that the contribution of the non-catalyzed reactions is negligible, at least under the reaction conditions used in this work. Preliminary experiments confirmed the results from previous works [28,29], showing that the catalytic activity of acid solids

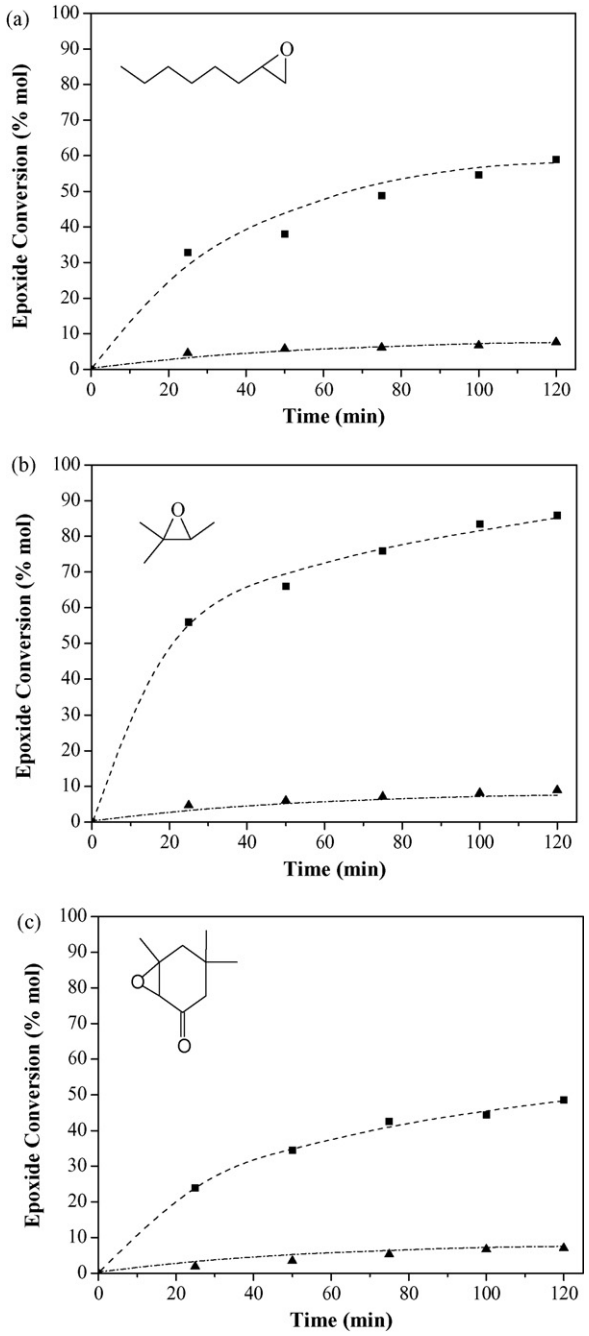

Fig. 3. Epoxide rearrangement conversion vs. reaction time: 1,2-epoxyoctane (a), 2-methyl-2,3-epoxybutane (b) and isophorone oxide (c). Temperatures: 150 °C, 80 °C and 80 °C, respectively. Catalysts: (■) n-ZSM-5, (▲) μ-ZSM-5.

for the rearrangement of branched and cyclic epoxides is quite higher than that obtained with linear epoxides, as a consequence of the lower reactivity of the latter. Accordingly, the reaction temperature for the rearrangement of 2-methyl-2,3-epoxybutane and isophorone oxide was set at 80 °C, whereas in the case of 1,2-epoxyoctane the reaction was carried out at 150 °C in order to obtain comparative epoxide conversions.

From the results shown in Fig. 3, it is concluded that in all cases the epoxide conversion over the μ-ZSM-5 zeolite reached hardly 10% after 2 h of reaction. In contrast, the epoxide conversion values obtained over the nanocrystalline ZSM-5 sample are considerable higher than those corresponding to the former, with values ranging about 40–80% at the end of the experiments. Both samples possess micropores with the same size, as well as a comparable amount of acid sites with a similar strength since their temperature maxima for ammonia desorption are placed around 350 °C. Therefore, the huge difference in the catalytic activity of both ZSM-5 samples must be attributed to their crystal size and external surface area.

In the case of the n-ZSM-5 sample the crystal size is in the nanometer range with a value almost two orders of magnitude lower than that of the μ-ZSM-5 material. This fact contributes favourably to the presence of an enhanced external surface area and, consequently, to a higher share of external acid sites, which are not limited by steric constraints as in the case of the acid sites located within the zeolite micropores.

Moreover, the overall diffusion rate through the micropores is inversely proportional to the square of the crystal size. Therefore, a quite higher intracrystalline diffusion rate should be expected for the n-ZSM-5 sample in regard to the ZSM-5 sample with a micrometer crystal size. The contributions of both factors causes an enhanced accessibility of the substrate molecules to the zeolite active sites, explaining the remarkable catalytic activity exhibited by the nanocrystalline ZSM-5 zeolite, which leads to high conversion, regardless the nature of the epoxide.

The high activity obtained in the rearrangement of 2-methyl-2,3-epoxybutane over n-ZSM-5 catalyst is remarkable, mainly when it is in compared with the conversion values obtained using a linear epoxide or a cyclic epoxide. After 2 h of reaction, the conversion of 2-methyl-2,3-epoxybutane over n-ZSM-5 is over 80%. It is well established that the acid-catalyzed reactions of epoxide rearrangement involves the initial attack of the electrophilic reagent to the oxirane ring, followed by the ring opening, yielding intermediate carbocations that subsequently may be transformed into the corresponding aldehyde and/or ketone [4]. The presence of branching in 2-methyl-2,3-epoxybutane epoxide and isophorone oxide provides a reactive tertiary carbon that favours the initiation step of the rearrangement reaction. Indeed, as a consequence of the high reactivity of the branched epoxides, 2-methyl-2,3-epoxybutane and α,β-epoxy ketone isophorone oxide, the processes were carried out at 80 °C, whereas the reaction temperature in the rearrangement of the linear epoxide had to be set at 150 °C in order to obtain significant conversions.

In addition to the different reactivity of the epoxide, and as it has been above indicated, the catalytic performance over n-ZSM-5 is also related to the overall accessibility of the substrate to the active sites, which is influenced by the possible presence of both steric and intracrystalline diffusion problems. Both factors depend on the zeolite properties (crystal size, micropore diameter and proportion of external surface area) but also on the geometry and effective size and of the epoxide molecules. In this way, Fig. 4 illustrates the molecular dimensions of the different epoxide molecules employed in this work, calculated at the reaction temperature by the Gaussian program [30]. The geometries of epoxide molecules were optimized using the 6-31G** basis set, at the ab initio DFT levels. The DFT calculation was carried out mainly with Becke's three-parameter exchange functional

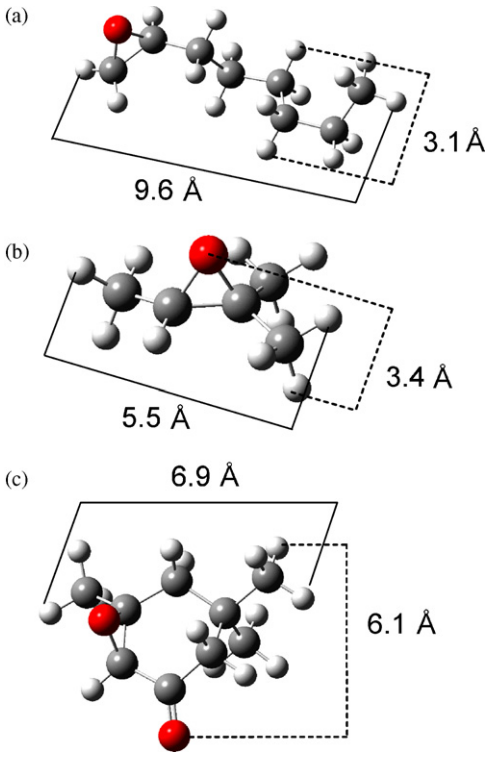

Fig. 4. Optimized geometry and selected dimensions for the epoxide molecules: (a) 1,2-epoxyoctane, (b) 2-methyl-2,3-epoxybutane and (c) isophorone oxide.

and the gradient-corrected functional of Lee, Yang, and Paar (B3-LYP hybrid functional) [31–33]. The results obtained show that the 2-methyl-2,3-epoxybutante molecule present dimensions of 3.4 × 5.5 Å, which are lower or very similar to the diameter of the ZSM-5 zeolite micropores. Therefore, it may be concluded that this molecule can enter the zeolite micropores, although having some limitations for diffusing across the zeolite channels. In the case of 1,2-epoxyoctane molecules, one of the dimensions is lower than the pore size whereas the other is clearly larger (3.1 × 9.6 Å, respectively). Accordingly, it may be assumed that this molecule may also enter the zeolite micropores, although suffering significant diffusion limitations. Finally, in the case of isophorone oxide, both dimensions (6.1 × 6.9 Å, respectively) are really larger than the pore size, which avoids its access to the active sites located within the zeolite micropores. Therefore, for this substrate the active sites are just those located on the external surface of the zeolite nanocrystals. The high conversion obtained with isophorone oxide should be related not just with the high reactivity of this epoxide but it confirms the important role played by the acid sites on the outer part of the zeolite crystallites.

Fig. 5 summarizes the molar product distribution obtained over both ZSM-5 samples in the liquid phase rearrangements of the three epoxides considered in this work. In all cases, the selectivities towards the main reaction products hardly vary with the course of the reaction. On the other hand, when analysing the differences observed between both catalysts, it should be taken into account that results corresponding to the ZSM-5 zeolite with micrometer crystal size may be strongly influenced by the low conversion obtained over this material.

Regardless the catalysts used, the main reaction products in the 1,2-epoxyoctane isomerisation were both octaldehyde and octen-1-ols, although other rearrangement products were also obtained. The appearance in the reaction product of 1,2-octanediol indicates the presence of some water, probably contained in the solvent and/or originated from the dehydroxylation of silanol groups

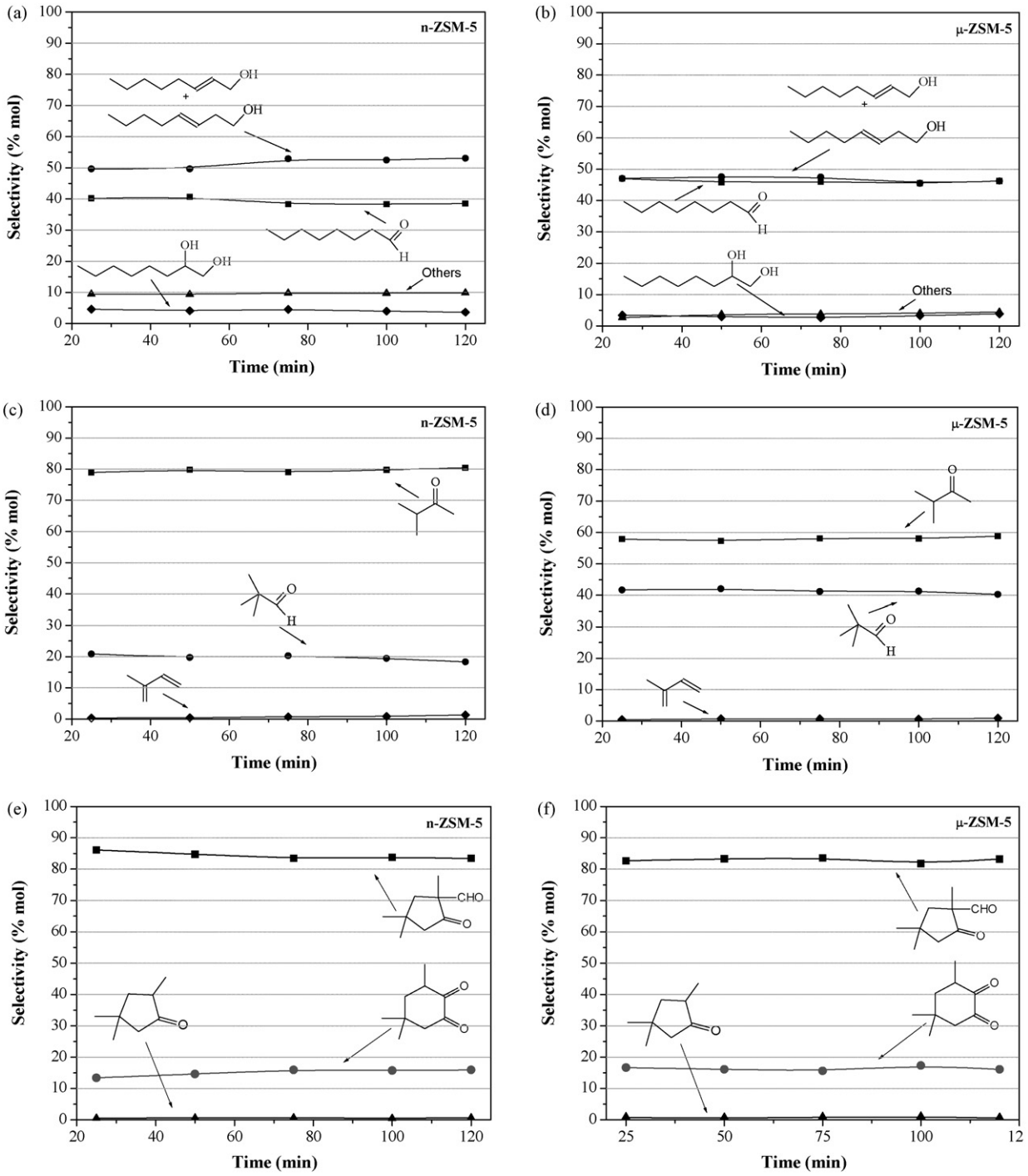

Fig. 5. Molar product distribution obtained in the epoxide rearrangement over ZSM-5 catalysts: (a, b) 1,2-epoxyoctane (150 °C), (c, d) 2-methyl-2,3-epoxybutane (80 °C), (e, f) isophorone oxide (80 °C).

located on the surface of the catalysts. The product distribution obtained over nanocrystalline ZSM-5 zeolite indicates that this type of catalyst favours the transposition of the positive charge of carbocations formed by the reaction mechanism [28], leading to an enhanced formation of octen-1-ols in regard to octaldehyde. Thus, over this catalyst the selectivity towards octen-1-ols is about 50%, whereas this parameter reaches a value around 40% in the case of octaldehyde. Nevertheless, taking into account that both of them are products with commercial interest, as they can be easily transformed into the corresponding terminal alcohol, the overall selectivity towards valuable products is over 90%.

Regarding to the molar product distribution obtained in 2-methyl-2,3-epoxybutane rearrangement (Fig. 5(c, d)), both catalysts lead to high selectivities towards methylisopropylketone, together with a considerable formation of 2,2-dimethylpropanal, whereas just a small proportion of isoprene is detected. These results can be explained considering that the ketone formation from the intermediate carbocation is favoured in comparison to its transformation to 2,2-dimethylpropanal or isoprene, as the latter involve methyl transposition and water loss steps, respectively [4]. For the nanocrystalline ZSM-5 zeolite, 2-methyl-2,3-epoxybutane isomerisation yields the formation of methylisopropylketone

with a really high selectivity (around 80%), whereas for 2,2-dimethylpropanal the selectivity was about 20%.

Finally, in the case of isophorone epoxide rearrangement, the main reaction product obtained was 2-formyl-2,4,4-trimethylcyclopentanone with selectivity around 80–85%, whereas the selectivity of 3,5,5-trimethyl-1,2-cyclohexanedione was set around 15%. These selectivity values are similar or even higher than those obtained in a previous work using Al-MCM-41 as a catalyst [29]. Consequently, these results indicate that over the ZSM-5 samples the presence of an additional substituent in the β-position of cyclic α,β-epoxy ketones, such as isophorone oxide, favours the acyl migration, resulting in ring contraction and consequently in the formation of the aldehyde. In contrast, hydrogen migration, leading to the α-diketone, takes place in a lesser extension. Moreover, acid sites in ZSM-5 zeolites do not promote the deformylation of 2-formyl-2,4,4-trimethylcyclopentanone, as demonstrated by the almost negligible selectivity towards 2,4,4-trimethylcyclopentanone obtained in this experiment.

In summary, the results obtained in the isomerisation of different epoxides over nanocrystalline ZSM-5 can be considered of high interest, since high catalytic activity and conversions are attained, whereas the catalyst exhibits also a high selectivity towards products with commercial applications. This can be explained by the presence of a high accessibility to the active sites in this catalyst, which favours the extension of the epoxide rearrangement reactions even when using large and/or low reactive epoxides.

4. Conclusions

The catalytic performance of nanocrystalline ZSM-5 zeolite in the liquid phase epoxide rearrangement in comparison to a microcrystalline ZSM-5 zeolite, employed as a reference catalyst, showed that the former presents remarkable catalytic properties, with both high epoxide conversions and high selectivity towards the desired products. The strong differences observed in the catalytic activity of both samples have been attributed to the enhanced accessibility of the epoxide molecules to the active sites in the case of nanocrystalline ZSM-5. This is a direct consequence of the small size of the crystals in this sample, which favours the intracrystalline diffusion process and provides a significant proportion of external surface area, the acid sites located on the latter being not limited by steric constraints. Likewise, for the sterically hindered epoxides, the catalytic rearrangement occurs on the external surface of the nanocrystalline zeolite.

The extent of the epoxide conversion was also dependent on the configuration of reactant molecule. Thus, the presence of branching in 2-methyl-2,3-epoxybutane epoxide and isophorone oxide provides a reactive tertiary carbon that favours the initiation step of the rearrangement reaction. Accordingly, whereas for those epoxides the catalytic tests were carried out at 80 °C, in the case of the rearrangement of the linear epoxide (1,2-epoxyoctane) the reaction had to be carried out at 150 °C in order to obtain comparative epoxide conversions.

In all cases, just slight changes were observed in the product distribution along the reaction time. As a consequence, it has been possible to obtain simultaneously high conversions and selectivities when using the n-ZSM-5 catalysts. While the conversions after 2 h of reaction ranged between 40 and 80%, the selectivities towards the desired products were over 80%. These remarkable results show the excellent catalytic properties exhibited by the nanocrystalline ZSM-5 in the isomerisation of different types of epoxides.

References

[1] J. March, Advanced Organic Chemistry, John Wiley, New York, 1992.
[2] J.G. Buchanan, H.Z. Sable, Selective Organic Transformations, Wiley, New York, 1972.
[3] S.M. Waqui, J.P. Horowitz, R. Filler, J. Am. Chem. Soc. 79 (1957) 6283.
[4] W.F. Hölderich, in: R.A. Sheldon, H. van Bekkum (Eds.), Fine Chemicals through Heterogeneous Catalysis, Wiley/VCH, Weinheim, 2001, p. 217.
[5] V.S. Joshi, N.P. Damodaran, S. Dev, Tetrahedron 27 (1971) 459.
[6] V.S. Joshi, S. Dev, Tetrahedron 33 (1977) 2955.
[7] P.B. Venuto, P.S. Landis, Adv. Catal. 18 (1968) 259.
[8] T. Imanaka, Y. Okamoto, S. Teranishi, Bull. Chem. Soc. Jpn. 45 (1972) 3251.
[9] S. Matsumoto, M. Nitta, K. Aomura, Bull. Chem. Soc. Jpn. 47 (1974) 1537.
[10] M. Nitta, S. Matsumoto, K. Aomura, J. Catal. 38 (1975) 498.
[11] G. Paparatto, G. Gregorio, Tetrahedron Lett. 29 (1988) 1471.
[12] W.F. Hölderich, H. van Bekkum, Stud. Surf. Sci. Catal. 137 (2001) 821.
[13] M. Chamoumi, D. Brunel, P. Geneste, P. Moreaus, J. Solofo, Stud. Surf. Sci. Catal. 59 (1991) 573.
[14] D.P. Serrano, M.A. Uguina, G. Ovejero, R. van Grieken, M. Camacho, Micropor. Mater. 4 (1995) 273.
[15] T.-L. Ho, S.-H. Liu, Synth. Commun. 13 (1983) 685.
[16] M. Asaoka, S. Hayashibe, S. Sonoda, H. Takei, Tetrahedron 47 (1991) 6967.
[17] C. Meyer, W. Laufer, W.F. Hölderich, Catal. Lett. 53 (1998) 131.
[18] M.J. Faraj, US Patent 5 312 995 (1993), to Arco Chemical Technology.
[19] W.F. Hölderich, N. Götz, L. Hupfer, H. Lermer, US Patent 4 980 511 (1987), to Basf AG.
[20] D. Brunel, M. Chamoumi, P. Geneste, P. Moreau, J. Mol. Catal. 79 (1993) 297.
[21] G.D. Yadav, D.V. Satoskar, J. Chem. Technol. Biotechnol. 69 (1997) 438.
[22] D.P. Serrano, J. Aguado, J.M. Escola, J.M. Rodriguez, J. Anal. Appl. Pyrolysis 74 (2005) 353.
[23] A. Corma, J. Catal. 216 (2003) 298.
[24] K. Wang, X. Wang, Micropor. Mesopor. Mater. 112 (2008) 187.
[25] J.L. Guth, H. Kessler, R. Wey, Stud. Surf. Sci. Catal. 28 (1986) 121.
[26] R. van Grieken, J.L. Sotelo, J.M. Menéndez, J.A. Melero, Micropor. Mesopor. Mater. 39 (2000) 135.
[27] B.C. Lippens, J.H. De Boer, J. Catal. 4 (1965) 319.
[28] D.P. Serrano, R. van Grieken, J.A. Melero, A. García, Appl. Catal. A: Gen. 269 (2004) 137.
[29] R. van Grieken, D.P. Serrano, J.A. Melero, A. García, J. Catal. 236 (2005) 122.
[30] M.J. Frisch, et al., Gaussian 03, Gaussian, Inc., Wallingford CT, 2004.
[31] C. Lee, W. Yang, R.G. Parr, Phys. Rev. B 37 (1988) 785.
[32] A.D. Becke, J. Phys. Chem. 98 (1993) 5648.
[33] P.J. Stephens, F.J. Devlin, C.F. Chabalowski, M.J. Frisch, J. Phys. Chem. 98 (1994) 11623.